Biomass Conversion and Biorefinery
https://doi.org/10.1007/s13399-024-06092-1

ORIGINAL ARTICLE

Extraction and characterization of biofiber from the *Phoenix sylvestris* leaf sheath biowaste for probable reinforcement in polymer composites

Aravind Ambika Gangadharan[1] · Rajesh Resselian[1] · Dev Anand Manoharan[1]

Received: 22 June 2024 / Revised: 13 August 2024 / Accepted: 26 August 2024

Abstract

In order to solve sustainability issues with its processes and products, the composites sector is concentrating on bio-waste as a different origin of materials for manufacture. The properties of *Phoenix sylvestris* leaf sheath fiber (PSLSF), a unique agro-waste that is separated from the tree's leaf sheath, was discussed in this paper. The *Phoenix sylvestris* leaf sheaths were collected from the *Phoenix sylvestris* tree locations and soaked in water to loosen the fiber. After 3 days of soaking the *Phoenix sylvestris* leaf sheaths were washed in running water to segregate the PSLSFs. The comprehensive analysis yielded quantitative information on PSLSF, including its tensile strength (192–239 MPa), Young's modulus (1.6–4.3 GPa), improved crystallinity index (53.6%), and cellulose proportion (64.43 wt%). Differential scanning calorimetry (DSC) and thermogravimetric (TGA/DTG) investigations shed light on the thermal stability of PSLSF and showed it durability up to 242 °C. Fourier transform infrared spectroscopy (FTIR) evaluation is used to verify the results of chemical assessment. An examination on the exterior texture of PSLSF employing scanning electron microscope (SEM) provided evidence to support the concept of utilizing it as a reinforcing component in composite with substrate as polymers. Research findings indicate that structural applications can benefit from the usage of PSLSF augmented polymeric composite.

Keywords Natural fiber · Sustainable · Chemical characterization · Reinforcement material · Biodegradable

Highlights.

Phoenix sylvestris leaf sheath fiber (PSLSF) proposed as reinforcement for polymer composites.

High cellulose content (64.63 wt%) noticed in PSLSF by chemical composition test.

Rough exterior surface of PSLSF promotes good interlocking while embedded in polymer matrix.

Tensile strength (192–239 MPa) and density (1.47 g/cm^3) exposes specific mechanical features.

Assessed CI value 53.6% approves the passable hydrophobic nature of PSLSF.

✉ Aravind Ambika Gangadharan
aravindag2021@gmail.com

[1] Department of Mechanical Engineering, Noorul Islam Centre for Higher Education, Kumaracoil 629180, Tamil Nadu, India

1 Introduction

Being sustainable in industrial operations is the norms due to ecological imbalances, which show themselves as a worldwide climatic change, contamination of water, air and earth, and depletion of ecological sources [1, 2]. Regulations were additionally implemented to promote environmentally friendly methods in order to protect and preserve the environment and its biodiversity. Any sector that wants to employ environmentally friendly practices needs to be very selective about the raw resources it utilizes [3]. Several sectors had either not started using environmentally friendly techniques yet or had just begun to use them. The composite industry was among the earliest to adopt environmentally friendly procedures, and its early endeavors were fruitful. This makes it possible for the composite sectors to continue operating and producing their goods effectively. Composite firms sought for ecologically friendly and decomposable raw materials to begin their sustainable approach [4]. The composite enterprises would benefit from the implementation of environmentally

Published online: 12 September 2024

friendly manufacturing procedures if they could find the perfect base material [5]. The fiber derived from minerals, animals, and plants remains the main choice available to composite producers. The persistent needs of the composite sectors cannot be met by animal-based fibers, and the cost of harvesting mineral fibers is higher [6]. Plant fibers may be a more common ingredient used by composite producers in countries with high levels of vegetation, such as India.

Fibers extracted from plants offer several advantages, such as easily biodegradable, low price, abundant prevalence, and less requirement of energy and hazardous intensive processing techniques; however, there are certain obstacles to overcome in order to optimize the composite's properties when organic yarns are utilized as support material in composites [7]. Meanwhile, these yarns have to be extracted straight away from ecosystem; it is impossible to control their physical form. Since the aforementioned fibers have different geometric shapes, the manufacturer finds it challenging to develop certain properties for composites composed of polymers employing these fibers as reinforcement material [8]. Furthermore, the availability of fibers that are natural is unable to managed based on needs since they come from natural sources. Alternative environmental risk expected is loss of forest area if fibers from trees were removed to cater the market needs [9]. However, some naturally fiber rich waste from agriculture is burned in open air, causing air pollution, or it is dumped in trash dumps, where it emits a foul stench over the neighborhood [10–12]. Composite enterprises that take advantage of these agricultural wastes rich in fiber create a circular economy that benefits farmers. Composite enterprises that take advantage of these waste products from agriculture packed with fiber establish an economic cycle that is beneficial to agriculturalists.

The properties of natural fibers that composite enterprises require depend on a variety of factors, including the organic nature of the material, the climate in which the tree or plant is cultivated, the oldness of the plants, and the portion of the herb or tree from which the yarn is harvested. The quality of the fibers is also influenced by the process used to extract it from the source material. Antony et al. [13] extensively characterized the leaf sheath fibers extracted from *Licuala grandis* tree. The tested yarns had a cellulose proportion of 49.13 wt%, tensile strength of 179 MPa, and with crystallinity index of 48%. The thermal stability of the fibers ensured through experiments ensures its use in composite industries. Manish et al. [14] explored the possibility of using fibers from leaf sheath of areca as sound absorbing material. They observed that the sound absorption capability of the areca leaf sheath fibers prepared as samples varied based on its thickness. The noise reduction coefficient was optimum for a 54-mm-thick sample, and it further increased by the introduction of air gap. With the 54-mm-thick areca leaf sheath sample and airgap of 20 mm, the noise reduction coefficient enhanced from 0.69 to 0.74.

Sekar et al. [15] characterized the leaf sheath fibers extracted from areca tree to know its possible utilization in industries. The fibers had a cellulose content of 56.8 wt%, tensile strength of 401 MPa, and with crystallinity index of 56.5%. The thermal stability was found to be 270˚C, and they suggest the leaf sheath fibers extracted from areca tree to be employed in textile sectors. The leaf sheath fibers extracted from windmill palm tree were investigated by Jing et al. [16] to know its suitable application in composite industries. The interrogated fibers showed a less cellulose content of 35.5 wt%, tensile strength of 132 MPa, and high micro fibril angle of 38.8 with comparable crystallinity index of 49.2%. But the elongation at break is 17.6% with the findings; the authors does not suggest any specific applications. Lami [17] investigated the effect of degumming process using alkali on the leaf sheath fibers extracted from palm tree. The author claims that the degumming process of leaf sheath fibers extracted from palm tree using alkali, hydrogen peroxide as bleaching agent, and silicone as softener improved its mechanical and moisture absorption characteristics.

The palm tree *Phoenix sylvestris* L., also known as the silver date palm in the local dialect, is a member of the Arecaceae family and is planted for its food, medicinal, and ornamental use. In Asian nations, *Phoenix sylvestris* is found growing in plains and scrublands. Its fruit is used to make pastries and wine. Following fruit harvesting, the leaf sheath remains as agro-wastes. Its trunk is used to make wooden gadgets for household applications. But the leaf sheath of *Phoenix sylvestris* L. is left out as waste which remains in landfills. The leaf sheath of *Phoenix sylvestris* L. contains enormous quantity of fibers which currently goes as waste. In a view to utilize *Phoenix sylvestris* leaf sheath fiber (PSLSF) in composite industries, the characteristics of the fiber was interrogated holistically. The PSLSF was exposed to physio-chemical and thermal testing to illustrate their mechanical, thermal, and chemical properties. SEM was utilized to assess the PSLSF's surface characteristics. XRD, TGA/DTG, and FTIR interrogations were performed on the PSLSF to evaluate its crystalline, thermal endurance, and functional groups, correspondingly. The most effective waste elimination plan may be developed, and the thermo-mechanical features of composite made of polymers can be enhanced by using PSLSF as a reinforcing material, according to studies on the material.

2 Materials and methods

2.1 Separation of PSLSF

The leaf sheaths belonging to *Phoenix sylvestris* was gathered from the garbage of corporate and educational sites in

and around Chennai, Tamil Nadu, India. The collected leaf sheaths shown in Fig. 1 were soaked in water for 3 days. The soaked leaf sheaths were washed in flowing water 5 or 6 times to separate the PSLSF from the pulp and remove other dust particles [18]. The extracted PSLSF were sundried to diminish its dampness content and stored for further study. The PSLSF was subjected to physical, mechanical, chemical, and thermal evaluations to ensure its suitability for usage as reinforcing material in composite industries.

2.2 Characterization of PSLSF

The chemical constituents of the PSLSF were explained using the standard techniques found in the scientific field, such as Krusher–Hoffer method for cellulose, the Conrad method for wax, the Klason method for lignin, and the Standard NFT 12–008 method for hemicellulose [19]. Using the ASTM E1755-61 norm, the amount of moisture in the PSLSF was ascertained. The density of PSLSF was computed by means of the mass-volume method. For this use, a known-volume container is stuffed with a powdered dry specimen of PSLSF and squeezed until all of the air is extracted. To calculate the fiber mass density, the weight of the container is recorded both with and without the powdered PSLSF specimen. Single fiber tensile test based on ASTM D3822-07 was conducted on PSLSF to assess its strength [20]. In every instance, ten specimens were examined. Using 4 cm^{-1} precision and 32 scans per minute, FTIR analysis was performed on PSLSF to determine the manifestation of functional clusters in the yarn. XRD spectroscopy was also performed on PSLSF using an upward goniometer displacement of 5°/min to show the XRD band over the Bragg angle (2θ) array of 10° to 80° using copper-K-alpha 1.54 Ang as the source of radiation [21]. The simplest method for comprehending the PSLSF's external features was to examine them using SEM images at an 8 kV accelerated voltage. The thermal durability of PSLSF was elucidated using TGA/DTG and DSC investigations, which entailed heating specimens to 550 °C and 450 °C, correspondingly, at a speed of 10 °C/min [22].

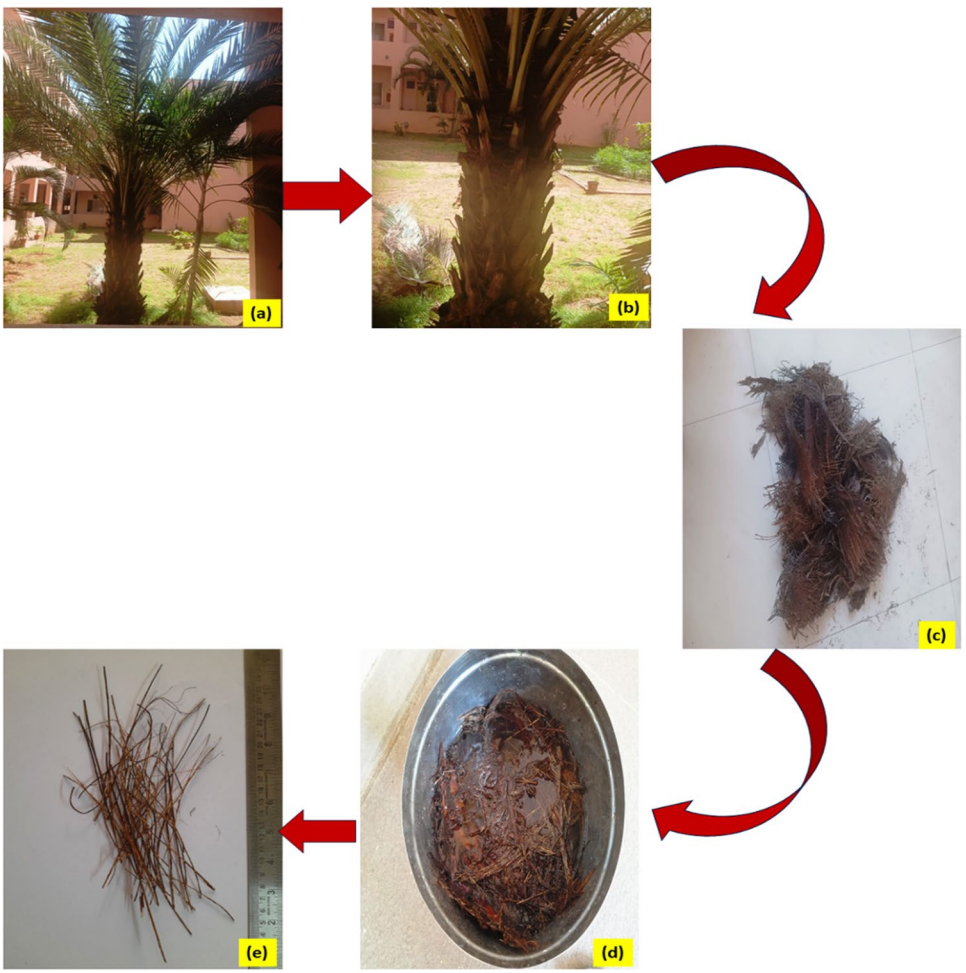

Fig. 1 Separation of *Phoenix sylvestris* tree leaf sheath fiber. **a** *Phoenix sylvestris* tree. **b** *Phoenix sylvestris* tree showing leaf sheath. **c** Collected leaf sheath of *Phoenix sylvestris* tree. **d** Water retting of collected leaf sheath. **e** Extracted *Phoenix sylvestris* tree leaf sheath fibers

3 Results and discussions

3.1 Chemical examination of PSLSF

The chemical properties of natural yarns are influenced by the growth environment of shrubs and trees, the age of the vegetation, and the parts of the herb that is used when the fiber is extracted. Environmental fiber's chemical composition can be utilized to infer specifics about their physio-mechanical, exterior texture, and crystallographic properties. The organic fiber's exterior texture has a major impact on the mechanical characteristics of the bonded polymeric composite [23]. Furthermore, the properties of the impregnated fibers have a significant influence on the features of vegetative fiber impregnated polymer composites. The chemical properties of PSLSF are presented as proportions of weight (wt%) in Table 1. The substantial percentage of 64.43 weight percent cellulose in PSLSF, that is equivalent with that of its substitutes, affects the mechanical features of the fiber. The crystalline form of PSLSF is aided by the substantial cellulose content, producing enough hydrophobic features for the yarn to be utilized as reinforcing substance in composites made of polymers.

On utilizing as reinforcements in polymeric composite materials, the PSLSF's minimum hemicellulose content of 10.36 weight percentage enhances the yarn's morphological and interaction features. On applying as reinforcements in composite with polymers as the base material, the 13.2 content % of lignin in the PSLSF functions as an adhesive and encourages contact with the substrate [24]. The fire-proofing of the PSLSF is attributed to its 1.5 weight percent ash content. If utilized as reinforcing substance in polymeric composite materials, the PSLSF's thermal endurance to withstand deterioration at polymerization heat is further strengthened by the ash content. Its application as reinforcements in composites made of polymers is supported by the acceptable weight proportions of wax (0.21 wt%) and dampness (10.3 wt%).

3.2 FTIR analysis of PSLSF

The FTIR findings of PSLSF are presented visually and tabulated in Fig. 2 and Table 2, respectively. The chemical architecture of PSLSF is shown by the FTIR spectrum. Chemical identification is aided by the distinct spectral patterns that each molecule produces. The visual plot provides insight into the presence of significant functional categories in the PSLSF. The valley that fluctuates at an oscillation rate of 1093 cm^{-1} is caused by an organic chemical cluster known as an alkyl halide [26]. The narrow valley perceived at a wavelength of 1389 cm^{-1} is caused by the wavy alkene group, a different organic functional cluster represented by = C-H. The apparent discrepancies in the FTIR graph up to 1493 cm^{-1} warrant the presence of sparsely distributed carboxylic group in

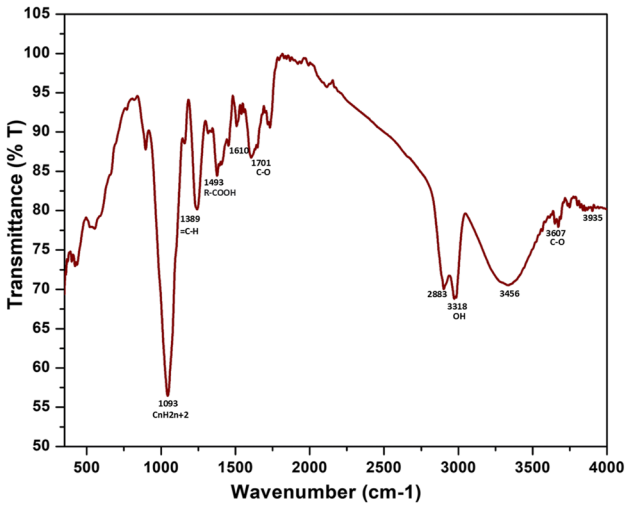

Fig. 2 FTIR spectrum of *Phoenix sylvestris* leaf sheath fiber

Table 1 Physical, chemical, and mechanical characteristics of *Phoenix Sylvestris* leaf sheath fiber in contrast with its ecofriendly counterparts [25]

Fiber name	Cellulose (wt%)	Hemicellulose (wt%)	Lignin (wt%)	Wax (wt%)	Density (g/cm^3)	Elongation at break (%)	Tensile Strength (MPa)	Young's modulus (GPa)
PSLSF*	**64.43**	**10.36**	**13.2**	**0.21**	**1.47**	**3.4–4.2**	**192–239**	**1.6–4.3**
Cissus quadrangularis stem	82.73	7.96	11.27	0.18	1.22	3.75–11.14	2300–5479	56–234
Areca fiber	57.35	13–15.42	23.17–24.16	0.12	0.7–0.8	10.23–13.15	147–322	1.12–3.15
Acacia leucophloea	76.69	3.81	13.67	0.13	1.43	1.91–5.88	357–1809	10.45–87.57
Nendran banana Peduncle fiber	73.20	10.85	15.32	0.25	0.97	2.17	65.51	49.50
Red banana peduncle fiber	72.90	11.01	15.99	0.32	0.89	1.97	40	12.41

Asterisk symbol represents the currently reported research work

Table 2 FTIR peak positions of *Phoenix sylvestris* leaf sheath fiber

Peak position in cm^{-1}	Allocation	Reference
1093	alkyl halide group	[26]
1389	=C-H stretch	[27]
1493	Carboxyl group	[27]
1701	Carbonyl functional group	[26]
2883	Occurrence of cellulose	[28]
3318	OH bond of hydrogen	[29]
3607	C-O stretch	[28]

Table 3 Physical entities of *Phoenix sylvestris* leaf sheath fiber

Property	Value
Primary cell wall thickness (µm)	1.59 ± 0.14
Secondary cell wall thickness (µm)	3.83 ± 0.35
Middle lamellae thickness (µm)	4.22 ± 0.28
Cell lumen thickness (µm)	9.85 ± 0.33
Fiber diameter (µm)	229.15 ± 18.57
Fiber density ($g{\cdot}cm^{-3}$)	1.45
Fineness (tex)	161 ± 9
Tenacity (g/tex)	21.24 ± 2.6

the PSLSF. The carbonyl operational group, denoted by C-O, is symbolized by the valley at 1701 cm^{-1} [27]. In the FTIR spectrum, undulations in the frequency of 2883 cm^{-1} indicate the presence of cellulose in the PSLSF. The broader valley shown at 3318 cm^{-1} in the FTIR spectrum of PSLSF is caused by the continuing presence of OH absorbed surrounding the cellulose. The alkali operational group predominates, which results in fluctuations around 3607 cm^{-1}, which signifies the symmetric expansion of C-O [28]. The insights from the FTIR study corroborate the findings of PSLSF's chemical examination.

3.3 Anatomical and morphological study of PSLSF

The physical features of the PSLSF, as seen by micro method to view the inner makeup of the yarn, are shown in Table 3. The cellulose and lignin that make up the PSLSF's primary and secondary cell walls, accordingly, significantly affect the mechanical properties of the fiber [29]. In the PSLSF, cells next to one another are joined by the lignin and hemicellulose adhering in the lamellae, which serve as tissues of connection. On utilizing as strengthening substance in composite made of polymers, the lumen, which is a void inside the PSLSF cells, enables the fibers from nature to retain a lower density and augments to the polymeric composite's lightweight quality.

Figure 3 depicts the PSLSF's external and cross-sectional perspectives as perceived by SEM. On utilizing as reinforcing component in polymeric composites, the coarse surface of the PSLSF, with its greater peak and valley, improves the interaction of the PSLSF with matrix, according to the findings from Fig. 3a [30]. The circumferential region of the boundary between the PSLSF and matrix is increased in the polymeric composite with reinforcing component that has greater peak and valley, which is beneficial for improving the bonding across interfaces. The mechanical properties of the PSLSF are further influenced by tiny fibrils that connect parenchyma cells and lignin, an organic substance that acts as a binding agent. The micro fibril angle well connected to the mechanical properties of the PSLSF. Utilizing Eq. (1), the micro fibril orientation of PSLSF is arrived to be 4.27° ± 0.13°:

$$\varepsilon = \ln\left[1 + \frac{\Delta L}{L_0}\right] = -ln(cos\alpha) \tag{1}$$

where ε is the strain, α is the micro fibril angle (degree), ΔL is the Elongation at break (mm), and L_o is the gauge length (mm). The computed micro fibril inclination is more in line with the 4.95° ± 0.32° estimate of the

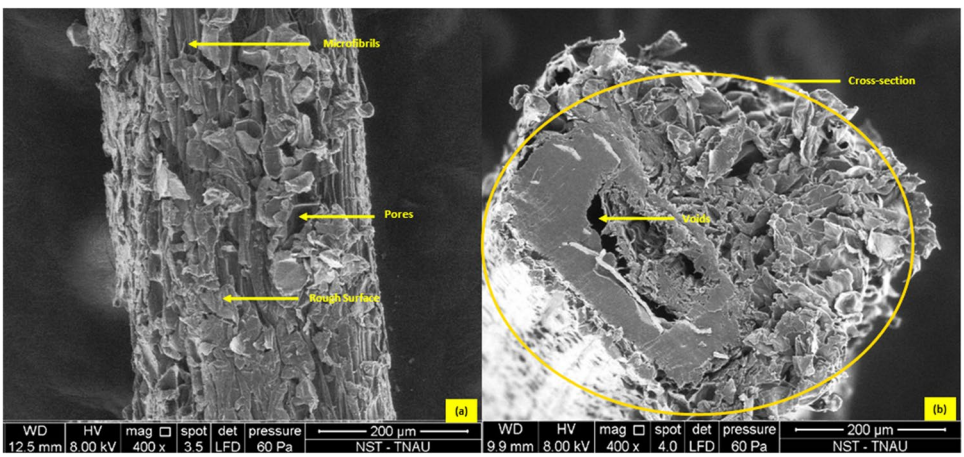

Fig. 3 SEM imageries of *Phoenix sylvestris* leaf sheath fiber: **a** surface view and **b** cross-sectional view

Cissus quadrangularis stem fiber [30]. When reinforced in polymeric composites, PSLSF's having low micro fibril angle enables the matrix and PSLSF to distribute stress appropriately.

3.4 XRD study of PSLSF

The XRD findings of PSLSF are shown graphically in Fig. 4. The crystalline characteristics of the PSLSF are understood from the pictorial representation. The partially crystalline properties of PSLSF are supported by the strong spike at Bragg angle (2θ) of 22.3° [31]. The prior small intensity spike found at 2θ of 16.7° is caused by the amorphous substances in the PSLSF. Regarding the crystalline elements of PSLSF, the larger spike at 22.3° of 2θ correlates to the crystallographic layer (2 0 0). The identified cellulose in this crystalline layer is categorized as cellulose-I and has a monoclinic structure. On the other hand, the amorphous substance spike of the PSLSF is located on the (1 1 0) crystallographic layer at 16.7° of 2θ. The PSLSF's crystallinity index (CI), as determined by Eq. (2) [32], was 53.6%.

$$\mathrm{CI} = \frac{(I_c - I_{am})}{I_c} \tag{2}$$

where I_c is the maximum intensity of crystalline peak at 2θ = 22.3° and I_{am} is the intensity of amorphous peak at 2θ = 16.7°. The analyzed CI number of the PSLSF guarantees that it possesses the requisite physical characteristics, such as crystallinity, to function as a reinforcing substance in composites made of polymers. Applying Scherrer's formula (3) [32], the crystallite size (CS) of the PSLSF was computed and arrived to be 3.13 nm.

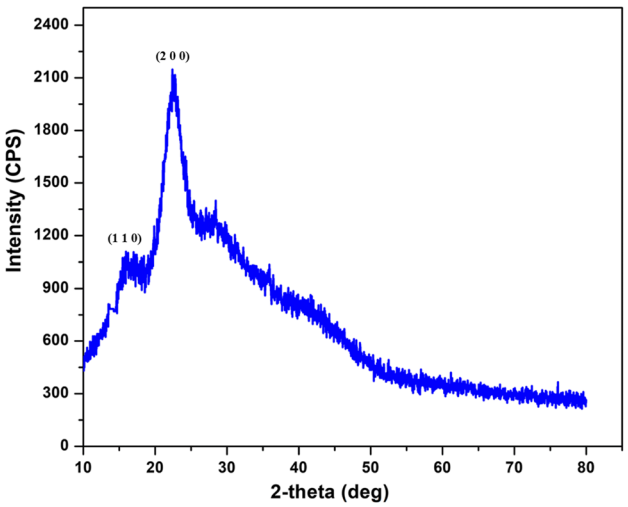

Fig. 4 XRD spectrum of *Phoenix sylvestris* leaf sheath fiber

$$\mathrm{CS} = \frac{K\lambda}{\beta cos\theta} \tag{3}$$

where K = 0.89 is Scherrer's constant, λ is the wave length of the radiation, β is the peak's full-width at half-maximum (FWHM) expressed in radians, and θ is the Bragg's diffraction angle. Table 4 displays PSLSF's CI and CS numeric in relation to other fibers found in the available research. The measured number of the CS amply supports its less hydrophilic nature, allowing PSLSF to be used as a reinforcement component in composites including polymers as the substrate.

3.5 Physico-mechanical study of PSLSF

Table 1 provides an overview of the PSLSF's physico-mechanical properties. Pulverized fibers were firmly stuffed in a tubular container of specified weight in order to calculate the PSLSF's density. The result was that the mass-volume density of the PSLSF was found to be 1.45 g/cm^3. When utilized as reinforcement, the natural fiber strengthened composite of polymers will have a lower density because of the PSLSF [33]. PSLSF strengthening contributes to the creation of materials with particular properties in polymer matrix composites. Employing image J software and an optical microscope, the diameter of the PSLSF was ascertained. Table 5 shows that the diameter of the PSLSF varied from 191.60 to 256.47 µm. Considering its irregular size and form, the PSLSF's cross-section is taken into consideration as round to facilitate the calculation of diameter using Eq. (4):

$$\mathrm{D_f} = \sqrt{\frac{L_f}{9000 \times M_d \times 0.7855}} \tag{4}$$

where D_f is the LGPF's diameter; L_f is its linear mass density in denier, which is a measure of the LGPF's fineness

Table 4 XRD outcomes of *Phoenix sylvestris* leaf sheath fiber in comparison with other fibers in the literature

Fiber	Crystallinity index (CI) in %	Crystallite size (CS) in nm	Reference
PSLSF	53.6	3.13	Present study
Purple bauhinia leaf fiber	54.98	2.8	[17]
Morinda tinctoria bark fiber	51	3.08	[27]
Ficus benjamina stem fiber	58.5	4.9	[15]
Cissus vitiginea stem fiber	30.5	12.69	[16]

Table 5 Mechanical characteristics of *Phoenix sylvestris* leaf sheath fiber

Gauge length (mm)	Tensile strength (MPa)	Young's modulus (GPa)	Strain to failure (%)	Diameter (μm)
10	192 ± 17	1.6 ± 0.2	4.2 ± 1.1	256.47 ± 21.34
20	208 ± 19	2.9 ± 0.4	4.0 ± 1.0	191.60 ± 16.37
30	223 ± 22	4.3 ± 0.8	3.7 ± 1.0	215.12 ± 17.65
40	233 ± 25	3.7 ± 0.6	3.4 ± 0.9	245.35 ± 19.26
50	239 ± 24	3.9 ± 0.6	3.5 ± 0.9	237.24 ± 18.38

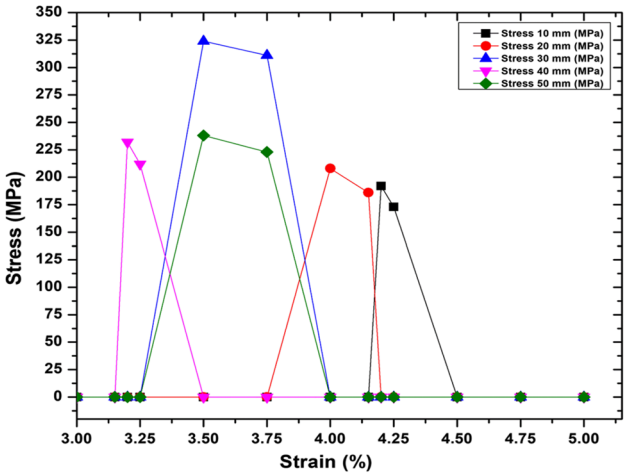

Fig. 5 Stress–strain curve of *Phoenix sylvestris* leaf sheath fiber

determined in accordance with ASTM D1577-07 standard; and M_d is its mass density in grams per cubic centimeter. The diameter of the PSLSF obtained from Eq. (4) is 223.81 μm, falling within the permitted range determined by using the image J software.

The PSLSF's tensile strength, which ranges from 192 to 239 MPa, is shown in Table 5 together with the stress–strain graph in Fig. 5. Similar to other plant-based fibers (such as Dorris scandens stem and the leaves of pineapple fiber) used as reinforcement in composites with polymers as the matrix, PSLSF shows equivalent tensile strength values [34–36]. There were five attempts at every experimentation. The PSLSF's cross-section, which varies in dimensions and shape throughout its span, is the reason for the discrepancy in physical properties observed along the gauge length change. The strain to failure estimates listed in Table 5 are supported by the PSLSF stress–strain graph shown in Fig. 5, which further highlights the examined fiber's fragility. The stress–strain curves start with the steep linear curve which is the elastic region of the PSLSFs. Following the elastic region, the PSLSFs exhibit a plastic region where the stress decreases and finally results in rupture of the PSLSFs showcasing a brittle failure. The higher Young's modulus and adequate elongation at break numerics of the PSLSF comprehend its exceptional load-withstanding ability [35]. The PSLSF can be used as reinforcing material in composites made of polymers due to its assessed and actual physico-mechanical features. Since organic yarns make up the majority of the load-bearing component of environmentally friendly composites made from fibers with polymers serving as the matrix, PSLSF with enhanced tensile features may be a suitable reinforcing substance.

3.6 TGA study of PSLSF

The PSLSF's thermal behavior was visually depicted in Fig. 6. The thermal endurance of the PSLSF is made clear by the graphic depiction. The PSLSF loses water as the temperature increases, as seen by the thermogravimetric profile, which indicates decreased mass of 6.1% up to 109 °C. Following dehydration of the PSLSF, the fiber sample exhibited satisfactory temperature endurance up to 242 °C, suggesting a 2.9% weight drop that signaled the start of the depolymerization phase [36]. The key component materials of the PSLSF, such as hemicellulose, lignin, and cellulose, initiated to decompose via the depolymerization process after a further increase in temperature. Up to 293 °C, this causes the PSLSF sample to lose mass by about 14.2%. The mass reduction of the PSLSF specimen in the temperature span of 294 °C to 378 °C indicates the complete cellulose disintegration in the processed fiber specimen [37]. The mass decrease that occurs after 379 °C designates that portion of the lignin and waxes has been detached from the extracted fiber sample.

The DTG graph variations show that the cellulose in the PSLSF suffers pyrolysis and molecular framework deterioration, with an acute point at around 331 °C and a mass difference of about 51.32%. The leftover char at 550 °C (15.57%) can be used to forecast the fire resistance of the PSLSF. The thermal properties of the PSLSF are shown in Table 6 together with those of different natural fibers found in the available literature. Using Broido's formula (5) [38], the kinetic activation energy (E) of the PSLSF was determined to be 72.36 kJ/mol. In Fig. 7, the Broido's graph was also displayed.

$$\ln\left[ln\left[\frac{1}{y}\right]\right] = -\left(\frac{E}{R}\right)\left[\left(\frac{1}{T}\right) + K\right] \tag{5}$$

where R is the universal gas constant (8.314 $J{\cdot}mol^{-1}K^{-1}$), T temperature in Kelvin, y normalized weight (w_t/w_o), w_t weight of the sample at any time t, w_0 initial sample weight, and k Boltzmann's constant ($1.3806 \times 10^{-23} J{\cdot}K^{-1}$). An important metric for assessing the PSLSF's capacity to facilitate polymerization in the process of creating polymeric composites is the estimated

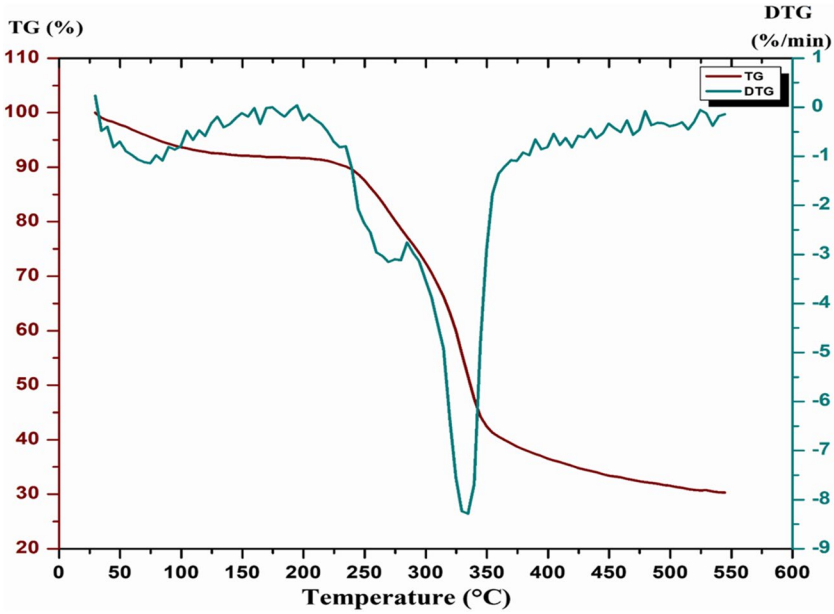

Fig. 6 TGA-DTG curve of *Phoenix sylvestris* leaf sheath fiber

Table 6 Thermal properties of *Phoenix sylvestris* leaf sheath in comparison with other natural fibers

Fiber	Glass transition temperature in °C	Degradation temperature in °C	Reference
PSLSF	242	378	Present study
Purple bauhinia leaf fiber	238	341	[17]
Morinda tinctoria bark fiber	240	330	[27]
Ficus benjamina stem fiber	233	336	[15]
Cissus vitiginea stem fiber	304	351	[16]

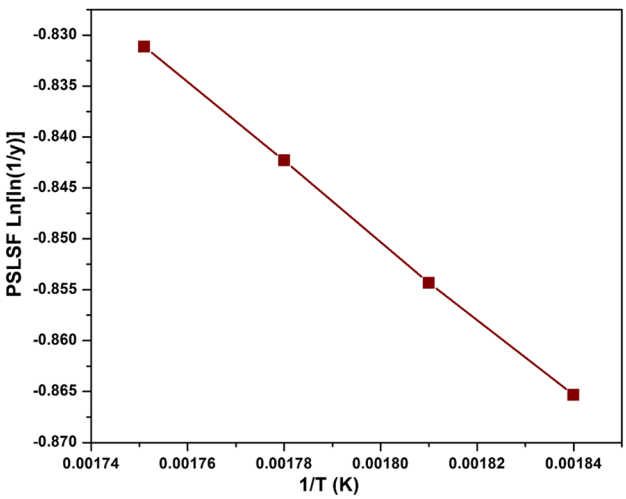

Fig. 7 Broido's plot of *Phoenix sylvestris* leaf sheath fiber

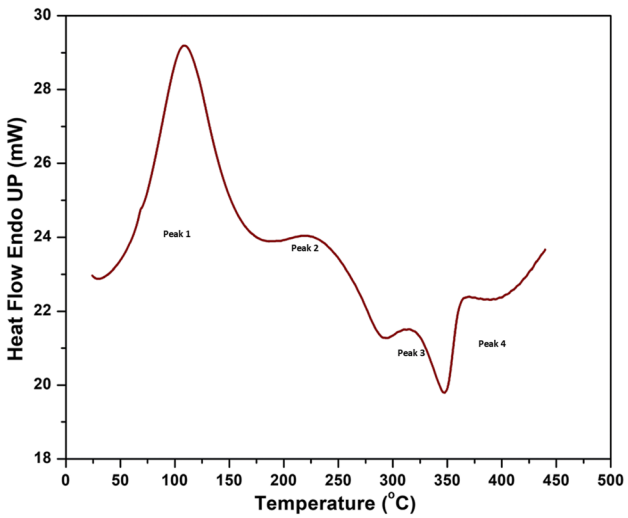

Fig. 8 DSC plot of *Phoenix sylvestris* leaf sheath fiber

E value. When the surrounding temperature is elevated, the utilization of PSLSF augmented composite polymers is supported by the PSLSF's thermal evaluations.

3.7 DSC study of PSLSF

The DSC results of PSLSF were visually displayed in Fig. 8. The visual representation shows the amount of heat transfer

across the PSLSF sample as the temperature increases. The DSC plot's endothermic curve illustrates how the cellulose-bound water molecule enables the PSLSF sample to lose wetness. The water particles that were firmly bonded in the cellulose of the PSLSF start to evaporate as temperatures get nearer to 100 °C [39]. The temperature of the PSLSF specimen subsequently rises even more, attaining 114.6 °C, which is the endothermic section of the DSC profile, where the dehydration of liquid droplets that are intimately adhered to cellulose takes place. The degradation of the wax in the PSLSF samples is designated by the exothermic profile at 169.7 °C [40]. The PSLSF specimen's damaged cellulose is due to the endothermic spike, which was detected at 223.6 °C. Pyrolysis is a process that occurs in hemicellulose and lignin, and it results in exothermic surges at 287.5 °C and 342.7 °C, correspondingly. At higher temperatures, further endothermic and exothermic fluctuations in the DSC profile indicate the lignin and hemicellulose degradation in the PSLSF [41]. The endothermic and exothermic variations observed in the PSLSF specimen after heating guarantee the use of PSLSF augmented composites of polymers in workplaces with greater ambient temperatures.

4 Conclusions

The outcomes of the PSLSF investigations clearly suggest that the composites sector will use this substance as a reinforcing agent in composites made of polymers. This initiates a more effective agro-waste administration strategy and assists composite companies in addressing sustainability issues with their products and processes. A 64.43 weight percent content of cellulose was found in the PSLSF after chemical analysis, favoring the mechanical properties required to be employed as a strengthening ingredient in composites using polymer as the substrate. The results of the chemical investigation were further supported by the FTIR evaluation that identified important functional compounds in the PSLSF. The density (1.45 g/cm^3) and tensile strength (192–239 MPa) of the PSLSF serve as examples of its exceptional mechanical qualities. It is confirmed that the PSLSF is adequately hydrophobic by the predicted CI number of 53.6%. High ambient temperature applications can benefit greatly from PSLSF integrated composites of polymers due to their endothermic and exothermic activity and thermal endurance up to 242 °C. The thermal and mechanical evaluations of PSLSF support the use of PSLSF enhanced polymer composites in frames that are lightweight under high ambient temperature circumstances. To determine the PSLSF strengthened polymeric composites' particular usefulness in sectors like building and automotive manufacturing, more research must be done on their characterization.

Author contribution A.A.G.: investigation (lead), resources and supporting. R.R.: writing-original draft, reviewing. D.A.M.: writing-original draft, reviewing.

Data availability This is an ongoing research work, and hence the data cannot be shared at this moment.

Declarations

Ethics approval and consent to participate All the authors demonstrate that they have adhered to the accepted ethical standards of a genuine research study. Also, individual consent from all the authors was undertaken to publish the data prior submitting to journal.

Consent for publication Written formal consent ensures that the publisher has the author's permission to publish research findings.

Competing interests The authors declare no competing interests.

References

1. A. Felix Sahayaraj, M. Tamil Selvan, M. Ramesh, J. Maniraj, I. Jenish, K. J. Nagarajan (2024) Extraction, purification, and characterization of novel plant fiber from *Tabernaemontana* divaricate stem to use as reinforcement in polymer composites. Biomass Conv Bioref https://doi.org/10.1007/s13399-024-05352-4
2. Manimaran P, Saravanan SP, Sanjay MR, Jawaid M, Siengchin S, Fiore V (2020) New lignocellulosic Aristida adscensionis fibers as novel reinforcement for composite materials: extraction, characterization and Weibull distribution analysis. J Polym Environ 28:803–811. https://doi.org/10.1007/s10924-019-01640-7
3. Bharath KN, Madhu P, Yashas Gowda TG, Sanjay MR, Kushvaha V, Siengchin S (2020) Alkaline effect on characterization of discarded waste of Moringa oleifera fiber as a potential eco-friendly reinforcement for biocomposites. J Polym Environ 28:2823–2836. https://doi.org/10.1007/s10924-020-01818-4
4. Lal HM, Uthaman A, Li C, Xian G, Thomas S (2022) Combined effects of cyclic/sustained bending loading and water immersion on the interface shear strength of carbon/glass fiber reinforced polymer hybrid rods for bridge cable. Constr Build Mater 314:125587. https://doi.org/10.1016/j.conbuildmat.2021.125587
5. Xian G, Zhou P, Bai Y, Wang J, Li C, Dong S, Guo R, Li J, Haoqiang Du, Zhong J (2024) Design, preparation and mechanical properties of novel glass fiber reinforced polypropylene bending bars. Constr Build Mater 429:136455. https://doi.org/10.1016/j.conbuildmat.2024.136455
6. Alshammari BA, Alotaibi MD, Alothman OY, Sanjay MR, Kian LK, Almutairi Z, Jawaid M (2019) A new study on characterization and properties of natural fibers obtained from olive tree (Olea europaea L.) residues. J Polym Environ 27:2334–2340. https://doi.org/10.1007/s10924-019-01526-8
7. A. Felix Sahayaraj, M. Tamil Selvan, I. Jenish, M. Ramesh (2023) Extraction and characterization of novel cellulosic fiber from Jatropha integerrima plant stem for potential reinforcement in polymer composites. Biomass Conv Bioref https://doi.org/10.1007/s13399-023-04541-x
8. Sumrith N, Laongdaw Techawinyutham MR, Sanjay RD, Siengchin S (2020) Characterization of alkaline and silane treated fibers of 'water hyacinth plants' and reinforcement of 'water hyacinth fibers' with bioepoxy to develop fully biobased sustainable ecofriendly composites. J Polym Environ 28:2749–2760. https://doi.org/10.1007/s10924-020-01810-y

9. Han X, Ding L, Tian Z, Song Y, Xiong R, Zhang C, Han J, Jiang S (2023) Potential new material for optical fiber: preparation and characterization of transparent fiber based on natural cellulosic fiber and epoxy. Int J Biol Macromol 224:1236–1243. https://doi.org/10.1016/j.ijbiomac.2022.10.209
10. Han X, Ding L, Tian Z, Weijie Wu, Jiang S (2021) Extraction and characterization of novel ultrastrong and tough natural cellulosic fiber bundles from manau rattan (Calamus manan). Ind Crops Prod 173:114103. https://doi.org/10.1016/j.indcrop.2021.114103
11. Srisuk R, Laongdaw Techawinyutham A, Vinod SM, Rangappa SS (2023) Agro-waste from Bambusa flexuosa stem fibers: a sustainable and green material for lightweight polymer composites. J Build Eng 73:106674. https://doi.org/10.1016/j.jobe.2023.106674
12. Thiagamani SMK, Nagarajan R, Jawaid M, Anumakonda V, Siengchin S (2017) Utilization of chemically treated municipal solid waste (spent coffee bean powder) as reinforcement in cellulose matrix for packaging applications. Waste Manag 69:445–454. https://doi.org/10.1016/j.wasman.2017.07.035
13. Britto ASF (2023) Joseph Selvi Binoj, Bright Brailson Mansingh & Paulvin Navin Jass, Extensive characterization of novel cellulosic biofiber from leaf sheath of Licuala grandis for biocomposite applications. Biomass Conv Bioref. https://doi.org/10.1007/s13399-023-04598-8
14. Raj M, Fatima S, Tandon N (2020) A study of areca nut leaf sheath fibers as a green sound-absorbing material. Appl Acoust 169:107490. https://doi.org/10.1016/j.apacoust.2020.107490
15. Das S, Chaudhuri A, Singha AK (2021) Characterization of lignocellulosic fibres extracted from agricultural biomass: arecanut leaf sheath. J Textile Institute 112(8):1224–1231. https://doi.org/10.1080/00405000.2020.1809319
16. Li J, Zhang X, Zhu J, Yan Yu, Wang H (2020) Structural, chemical, and multi-scale mechanical characterization of waste windmill palm fber (Trachycarpus fortunei). J Wood Sci 66(8):1. https://doi.org/10.1186/s10086-020-1851-z
17. Rajeshkumar G, Devnani GL, Prakash Maran J, Sanjay MR, Siengchin S, Al-Dhabi NA, Ponmurugan K (2021) Characterization of novel natural cellulosic fibers from purple bauhinia for potential reinforcement in polymer composites. Cellulose 28:5373–5385. https://doi.org/10.1007/s10570-021-03919-2
18. Khan A, Vijay R, Lenin Singaravelu D, Sanjay MR, Siengchin S, Jawaid M, Alamry KA, Asiri AM (2022) Extraction and characterization of natural fibers from *Citrullus lanatus* climber. J Nat Fibers 19:621–629. https://doi.org/10.1080/15440478.2020.1758281
19. Sudhir Chakravarthy K, Madhu S, Raju JSN, Jabihulla Shariff Md (2020) Characterization of novel natural cellulosic fiber extracted from the stem of Cissus vitiginea plant. Int J Biol Macromol 161:1358–1370. https://doi.org/10.1016/j.ijbiomac.2020.07.230
20. Standard Test method for tensile properties of single textile fibers (2010). Assessed on18.10.2023. https://www.astm.org/d3822-07.html
21. Senthil Muthu Kumar T, Yorseng K, Rajini N, Siengchin S, Ayrilmis N, Varada Rajulu A (2019) Mechanical and thermal properties of spent coffee bean filler/poly(3-hydroxybutyrate-co-3-hydroxyvalerate) biocomposites: Effect of recycling. Process Saf Environ Prot 124:187–195. https://doi.org/10.1016/j.psep.2019.02.008
22. Kumar TS, Rajini N, Huafeng T, Rajulu AV, Ayrilmis N, Siengchin S (2019) Improved mechanical and thermal properties of spent coffee bean particulate reinforced poly(propylene carbonate) composites. Part Sci Technol 37(5):643–650. https://doi.org/10.1080/02726351.2017.1420116
23. Siva SR, Valarmathi TN, Palanikumar K, Samrot AV (2020) Study on a Novel natural cellulosic fiber from Kigelia africana fruit: characterization and analysis. Carbohydr Polym 244:116494. https://doi.org/10.1016/j.carbpol.2020.116494
24. Manimaran P, Pitchayya Pillai G, Vignesh V, Prithiviraj M (2020) Characterization of natural cellulosic fibers from Nendran banana peduncle plants. Int J Biol Macromol 162:2131687. https://doi.org/10.1016/j.ijbiomac.2020.08.111
25. Manimaran P, Sanjay MR, Senthamaraikannan P, Mohammad Jawaid SS, Saravanakumar SS, R, George (2019) Synthesis and characterization of cellulosic fiber from red banana peduncle as reinforcement for potential applications. J Nat Fibers 16(5):768–780. https://doi.org/10.1080/15440478.2018.1434851
26. Muthukrishnan KM, Selvakumar G, Narayanasamy P, Ravindran P (2022) Characterization of raw and alkali treated cellulosic filler isolated from Putranjiva roxburghii W. seed shell roadside vegetative residues. J Nat Fibers 19(16):14287–14298. https://doi.org/10.1080/15440478.2022.2061670
27. French AD (2014) Idealized powder diffraction patterns for cellulose polymorphs. Cellulose 21:885–896. https://doi.org/10.1007/s10570-013-0030-4
28. Balachandran GB, Narayanasamy P, Alexander AB, David PW, Mariappan RK, Ramachandran ME, Indran S, Rangappa SM, Siengchin S (2023) Multi-analytical investigation of the physical, chemical, morphological, tensile, and structural properties of Indian mulberry (Morinda tinctoria) bark fibers. Heliyon 9(11):e21239. https://doi.org/10.1016/j.heliyon.2023.e21239
29. Selvaraj M, Akash S, Mylsamy B (2023) Characterization of new natural fiber from the stem of Tithonia Diversifolia plant. J Bionic Eng 20:2167144. https://doi.org/10.1080/15440478.2023.2167144
30. Indran S, Edwin Raj R (2015) Characterization of new natural cellulosic fiber from Cissusquadrangularis stem. Carbohydr Polym 117:392–399. https://doi.org/10.1016/j.carbpol.2014.09.072
31. Joseph Selvi Binoj, Mariatti Jaafar, Bright Brailson Mansingh, Govindarajan Bharathiraja (2023) Extraction and characterization of novel cellulosic biofiber from peduncle of Areca catechu L. biowaste for sustainable biocomposites. Biomass Conv Bioref https://doi.org/10.1007/s13399-023-04081-4
32. Segal L, Creely JJ, Martin AE Jr, Conrad CM (1959) An empirical method for estimating the degree of crystallinity of native cellulose using the x-ray diffractometer. Text Res J 29:786–794. https://doi.org/10.1177/004051755902901003
33. Palaniyappan Sabarinathan VE, Annamalai K, Rajkumar KV, Dhinakaran V (2022) Synthesis and characterization of randomly oriented silane-grafted novel bio-cellulosic fish tail palm fiber–reinforced vinyl ester composite. Biomass Conv Bioref 13(17):16067–16084. https://doi.org/10.1007/s13399-022-02459-4
34. Senthamaraikannan P, Kathiresan M (2018) Characterization of raw and alkali treated new natural cellulosic fiber from Coccinia grandis. L. Carbohydr Polym 186:332–343. https://doi.org/10.1016/j.carbpol.2018.01.072
35. Senthamaraikannan P, Saravanakumar SS, Sanjay MR, Jawaid M, Siengchin S (2019) Physico-chemical and thermal properties of untreated and treated Acacia planifrons bark fibers for composite reinforcement. Mater Lett 240:221–224. https://doi.org/10.1016/j.matlet.2019.01.024
36. Ilaiya Perumal C, Sarala R (2020) Characterization of a new natural cellulosic fiber extracted from Derris scandens stem. Int J Biol Macromol 165:2303–2313. https://doi.org/10.1016/j.ijbiomac.2020.10.086
37. Senthamaraikannan P, Saravanakumar SS (2022) Effect of Cocos nucifera shell powder on mechanical and thermal properties of Mucuna atropurpurea stem fibre-reinforced polyester composites. Biomass Conv Bioref 13:11275–11294. https://doi.org/10.1007/s13399-022-03621-8
38. Brailson Mansingh B, Binoj JS, Hassan SA, Mariatti M, Siengchin S, Sanjay MR, Bharath KN (2022) Characterization of natural cellulosic fiber from Cocos Nucifera peduncle for sustainable

biocomposites. J Nat Fibers 19:9373–9383. https://doi.org/10.1080/15440478.2021.1982827
39. Senthamaraikannan P, Saravanakumar SS (2023) Evaluation of characteristic features of untreated and alkali-treated cellulosic plant fibers from Mucuna atropurpurea for polymer composite reinforcement. Biomass Conv Bioref 13:11295–11309. https://doi.org/10.1007/s13399-022-03736-y
40. Thooyavan Y, Kumaraswamidhas LA, Edwin Raj R, Binoj JS, Brailson Mansingh B (2022) Failure analysis of basalt bidirectional mat reinforced micro/nano SiC particle filled vinyl ester polymer composites. Eng Fail Anal 136:e106227. https://doi.org/10.1016/j.engfailanal.2022.106227
41. Senthamaraikannan P, Saravanakumar SS (2023) Effect of Cocos nucifera shell powder on mechanical and thermal properties of Mucuna atropurpurea stem fibre-reinforced polyester composites. Biomass Conv Bioref 13:11275–11294. https://doi.org/10.1007/s13399-022-03621-8